

EXPERIMENTAL INVESTIGATION OF THE FRICTIONAL CONTACT IN PRE-SLIDING REGIME

Iuliana PISCAN¹

În această lucrare sunt investigate din punct de vedere experimental, caracteristicile contactului cu frecare în regimul de pre-alunecare. Pentru efectuarea măsurătorilor, un tribometru existent a fost utilizat. Curbele histerezis, determinate experimental, sunt reprezentate printr-un model parametric. Astfel, prin reprezentarea curbei histerezis caracteristice, rigiditatea de contact și amortizarea echivalentă au fost determinate. Rezultatele experimentale relevă un comportament tipic al curbei histerezis și un comportament previzibil al frecării. Coeficientul de frecare scade cu creșterea forțelor normale, în timp ce forța de frecare crește cu creșterea forțelor normale. Distanța de pre-alunecare crește odată cu creșterea forțelor normale.

This paper investigates the experimental study of the frictional contact characteristics during pre-sliding regime. For the experimental tests, a previously developed linear tribometer is used. The measured hysteresis loops are fitted using a parametric model equation. From the virgin curve expression, the contact stiffness and damping are determined. The experimental results describe a typical hysteresis curve and an expected frictional behaviour is confirmed. The friction coefficient shows a decreasing behaviour with the load in opposition with the friction force that is increasing with load. However, the pre-sliding distance is increasing with higher load.

Keywords: frictional contact, hysteresis, friction force, friction coefficient, contact stiffness, equivalent damping

1. Introduction

Frictional contacts have a nonlinear behaviour that can be found in almost any mechanical system with moving components. Contact has an important role in transmitting forces and/or torque in any mechanical systems. Therefore, the behaviour of structures or joints, e.g. bolted connection, flat on flat connection, guidelines are considerably influenced by the contact parameters.

Friction force is the result of relative motion of two or more contacting surfaces in tangential direction. Dry frictional contact depends on various factors such as the applied load, surface topography, sliding velocity, temperature, elastic and plastic properties, material of frictional surfaces and displacement of the bodies in contact [1]. The most important characteristics of friction that occur

¹ PhD. student, Machines and Production Systems Department, University POLITEHNICA of Bucharest, Romania, e-mail: iuliana.piscan@yahoo.com

during the process of friction are the hysteretic effects. The hysteretic effect can be perceived during sticking and sliding phases being caused by the behaviour of friction force that acts as a nonlinear spring before sliding. This phenomenon, appearing at the microscopic level, is called pre-sliding displacement and is resulted from the tangential contact stiffness between contacting bodies [2, 3, 4, 5].

Numerous studies concerning contact problems with friction have been the subject of various experimental investigations for many years and recently numerous computational investigations have been performed.

The characterization of friction depends significantly on the accuracy of experimental measurements. The frictional behaviour is generally a characteristic of the system, and not only of the materials in contact, therefore no single test can describe all types of frictional situations [6].

Furthermore, studies have been made in relating the friction coefficient to contact parameters and relevant operating conditions through theoretical modelling [7, 8] though the most significant sources of guidance to practical values are experimental investigations [9, 10, 11].

This paper treats the experimental friction identification in the pre-sliding regime friction, which is predominantly position dependent (function of pre-sliding displacement) for a flat on flat connection.

The aim of these experiments was to determine the friction force and the relative displacement, x as a function of the normal load at different load cases, for different materials and to evaluate the breakaway force, the maximum attainable friction coefficient and the maximum stiffness. The experiments were limited to the pre-sliding regime, which is predominantly position dependent (function of the pre-sliding displacement). The normal load dependency is the most critical in this analysis.

In the pre-sliding (micro-slip) regime, the relative displacement between the two contacting surfaces is microscopic. The friction force in this regime is mainly a function of displacement, and is due to the adhesive forces derived from the asperity junction elasto-plastic deformation. As the displacement increases, more and more junctions break, and finally there is a breakaway displacement beyond which gross sliding (the sliding regime) begins [2].

2. The experimental procedure

The experimental investigation is carried out to determine the characteristics of the frictional contact. The measurements are performed on a previously developed tribometer [12] with some minor adjustments. Tribometers can be used for investigation of rolling or sliding friction in dry or lubricated contacts. In this paper, the used tribometer is for sliding friction in dry conditions.

By using this setup, when the upper body starts to slide on the lower body, the friction coefficient μ_s can be determined as a ratio between the friction force F_f and the normal load, W

$$\mu_s = \frac{F_f}{W} \quad (1)$$

The test geometries for these types of experiment can be classified into two main groups: conformal and non-conformal geometries as shown in Fig. 1. For the conformal geometry, a precise alignment of the two contacting surfaces is required and the contact pressure is uniformly distributed. The contact stresses, in non-conformal contact tests are varying with location in the region of contact during the experiments [13].

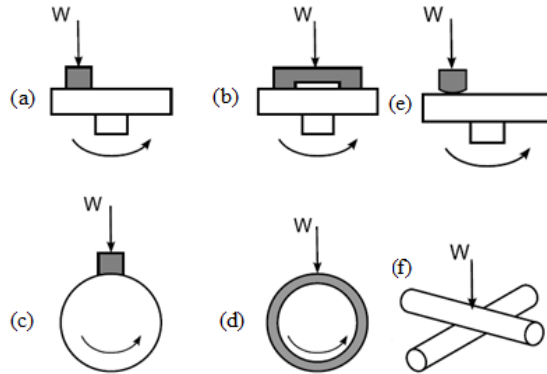


Fig. 1. Friction measurements using conformal geometries: a) flat pin on disc, b) thrust washer, c) pin on cylinder, d) shaft bush and non-conformal geometries: e) hemispherical pin on disc, f) crossed cylinder

Fig. 2 shows the conformal contact geometry and the two contacting bodies used in experiments, which makes contact in one surface. The lower body is supported by a moving block which makes contact with the upper body supported by the friction block, on which the friction force acts. Two displacement sensors measure the relative displacement of the two contacting bodies and the friction force is measured by a force cell.

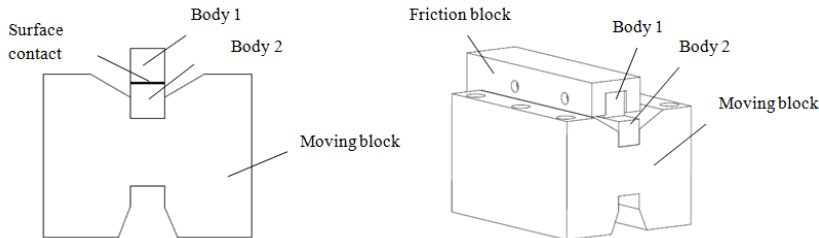


Fig. 2. Configuration of the contact geometry

Three material pairs are used for the experiments:

- Aluminium on aluminium;
- Plastic on plastic (PVC on PVC);
- Steel on steel;

The material pairs were used in the experimental investigation as a contact material because of their predominant applicability in many mechanical structures.

3. The experimental computation of hysteresis loops

The friction force F_f as a function of the relative displacements x , or the hysteresis loops, determined experimentally were averaged over the periods in order to eliminate noise and random behaviour effects. These curves are fitted using the exponential equation [14]:

$$F(x) = h_0(1 - e^{-a_c(x - x_0)}) \quad (2)$$

The parameters, h_0 and a_c are used to evaluate the results. The parameter x_0 , represents a variable which allows to shift the starting point of the hysteresis half towards the origin of the hysteresis. Other model equations are also possible [4]. Many experiments were performed for different normal load cases and for different displacement amplitudes, in order to determine the evolution of the frictional force as a function of the normal load, the contact stiffness and contact damping. The experiments are restricted to the pre-sliding regime.

3.1. Experimental results for aluminium on aluminium

The experimentally determined hysteresis loop and its fit for one material combination (Aluminium) is shown in Fig. 3.

The model parameters, h_0 and a_c , are used to describe the hysteresis behaviour. The first parameter h_0 , representing the saturation value of the hysteresis loop can be seen as the static friction force limit, or the breakaway force. The parameter a_c represents a measure of the curvature of the hysteresis, determining the shape of the curve and can be interpreted as follows: for higher values of a_c , the curve will be more convex and, therefore the dissipation per cycle will increase. These parameters are plotted in Fig. 4 as a function of the normal load. An increasing trend for h_0 can be noticed and the parameter a_c is decreasing with an increasing normal load. These trends are also observed in the experimental results described in [14], where the relation between the friction force and the normal load was investigated in pre-sliding up to sliding for three material contacts, e.g. steel on PET, PET on PET, steel on brass.

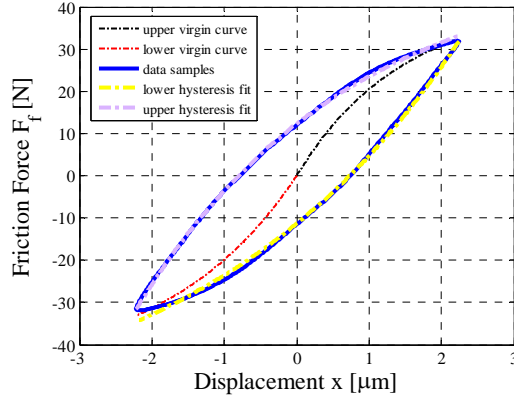


Fig. 3. Hysteresis in pre-sliding regime: aluminium on aluminium, $W = 109$ N, $f = 1$ Hz

In Fig. 4, these parameters are plotted as a function of the external normal load W . One can notice an increasing trend for h_0 , while the parameter for the curvature of the hysteresis a_c , decreases with an increasing normal load. In Fig. 5, the pre-sliding distance is plotted as a function of the normal load, which increases with increasing normal load.

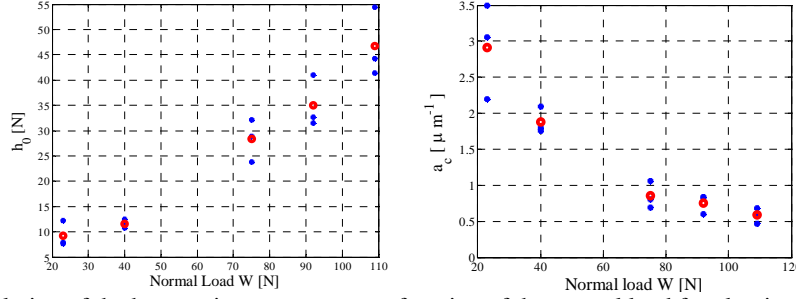


Fig. 4. Evolution of the hysteresis parameters as a function of the normal load for aluminum on aluminium

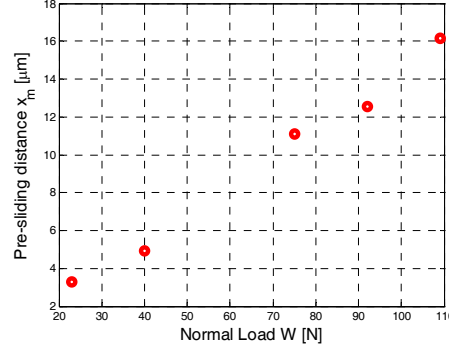


Fig. 5. Evolution of the pre-sliding distance as a function of the normal load

The evolution of the pre-sliding distance is described in Figure 5. The pre-sliding distance is defined such that $F \approx 0.99F_{breakaway}$ [14].

$$e^{-a_c x_m} = 0.01 \rightarrow x_m = \frac{-\ln 0.01}{a_c} \quad (3)$$

Based on the identification of the virgin curves, the pre-sliding coefficient of friction is plotted in Fig. 6 as a function of different normal loads and displacements that are extrapolated beyond the pre-sliding distance. For higher loads, the friction coefficient (h_0/W) is decreasing and the pre-sliding distance ($x_m \approx 1/a_c$) is increasing, where the blue dots represent the pre-sliding distance. An opposite trend is noticed in Fig. 7 where the friction force is increasing with increasing normal load.

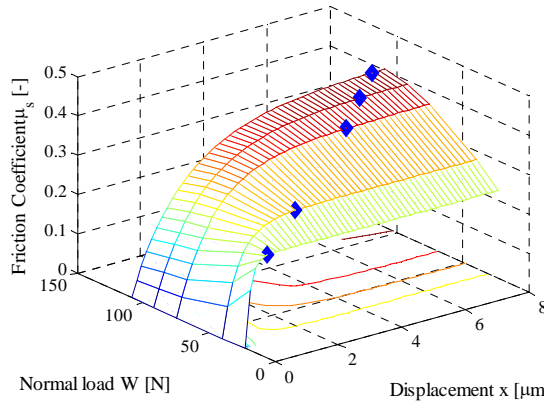


Fig. 6. Evolution of the friction coefficient for different load cases and displacements

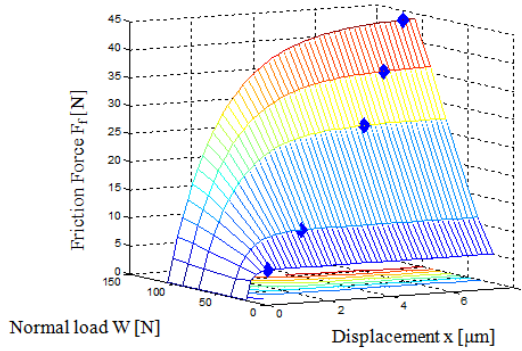


Fig. 7. Evolution of the friction force for different load cases and displacements

The equivalent contact damping $c_e \cdot \omega$ [$N/\mu m$], plotted in function of the normal load and displacement is shown in Fig. 8. The contact damping is increasing with higher normal load and decreasing with the increasing displacement after reaching a maximum.

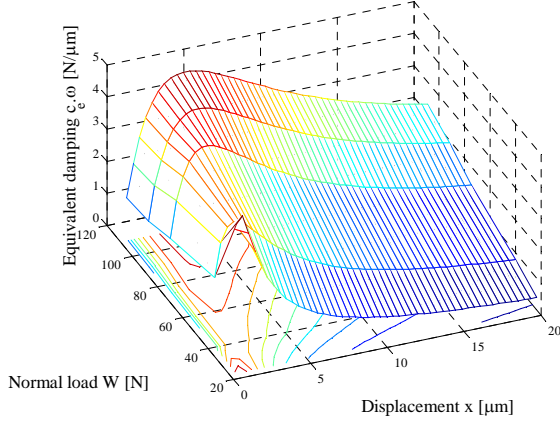


Fig. 8. Equivalent damping as a function of normal load and displacement

In Fig. 9 the global contact stiffness and, respectively, the local contact stiffness are shown. This figure shows that the stiffness is increasing with the load and weakening with the amplitude.

The difference between the two contact stiffnesses is the method of computation: the global contact stiffness (5) is the ratio between force and displacement and the local contact stiffness is the derivation of the virgin curve (4) (see related equations below):

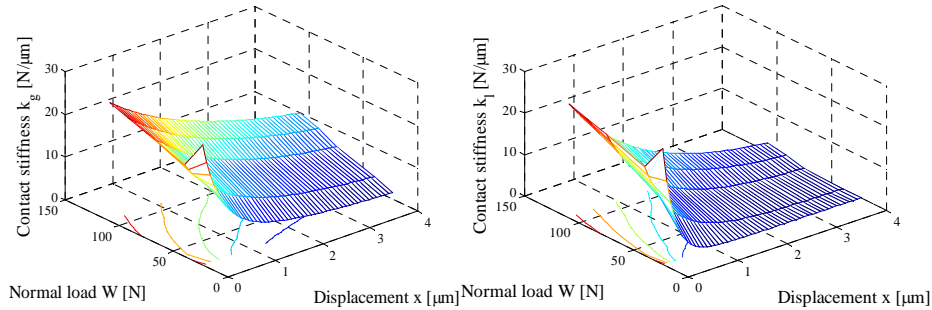


Fig. 9. Global stiffness and local stiffness as a function of normal load and displacement

$$k_l = h_0 \cdot a_c \cdot \exp(-a_c \cdot x) \quad (4)$$

$$k_g = \frac{h_{virg}}{x} \quad (5)$$

3.2. The experimental results for PVC on PVC

The results of the experiments with PVC are presented in this section. In Fig. 10, the amplitude and load dependency of the hysteresis loops are plotted for the same load with different amplitude and for different increasing amplitudes at different normal loads. This figure shows that the hysteresis curves are weakening as a function of amplitude and stiffening as a function of normal load. As it can be noticed, this contact material has a similar frictional behaviour as aluminium contact.

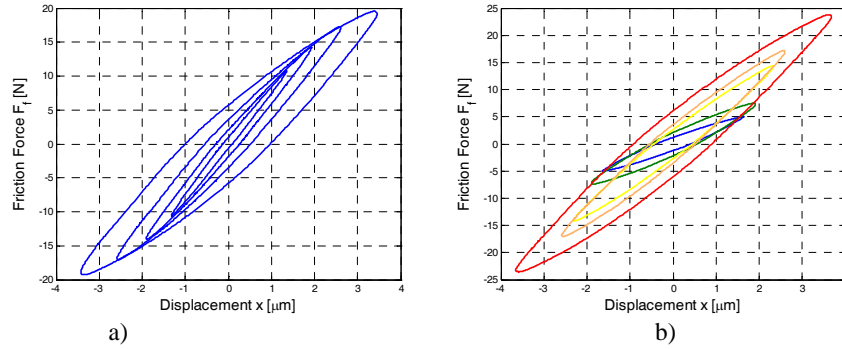


Fig. 10. The friction force F as a function of the displacement x : a) for the same loads with different increasing amplitudes; b) for different loads and different increasing amplitudes

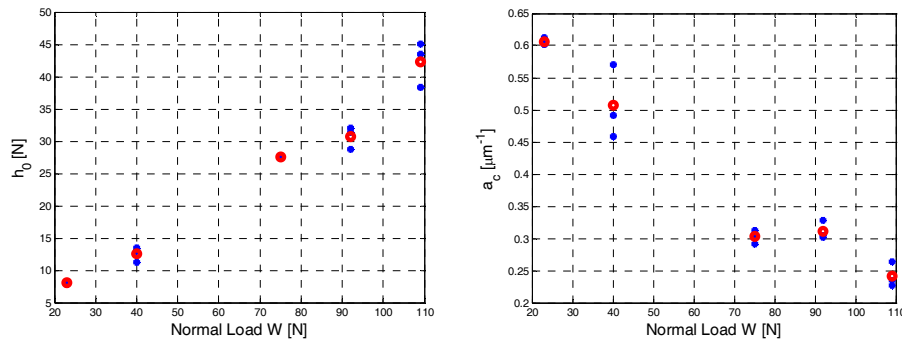


Fig. 11. Evolution of the hysteresis parameters as a function of the normal load for PVC on PVC

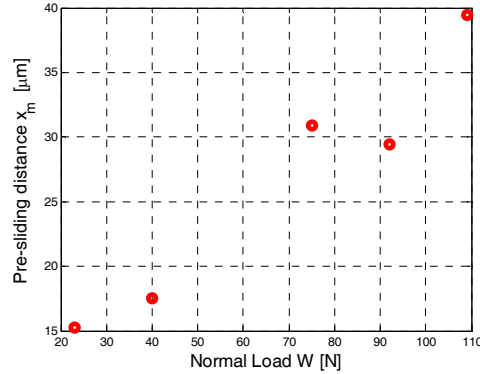


Fig.12. Evolution of the pre-sliding distance as a function of the normal load for PVC on PVC

In Fig. 11, the model hysteresis parameters h_0 and a_c are observed. A similar increasing trend for h_0 and decreasing trend for a_c as in the previous experiments is confirmed. The evolution of the pre-sliding distance is visualised in Fig. 12.

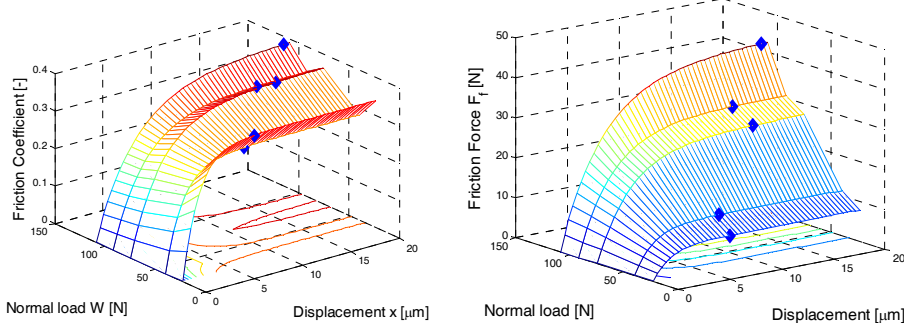


Fig. 13. The evolution of the friction coefficient and friction force as a function of normal load and displacement

The evolution of the coefficient of friction and friction force as a function of the normal load and displacement, are plotted in Fig. 13. Fig. 14 presents the equivalent contact damping as a function of the normal load and displacement.

In Fig. 15 are showed the local contact stiffness and global contact stiffness which have the same trend as for aluminium contact.

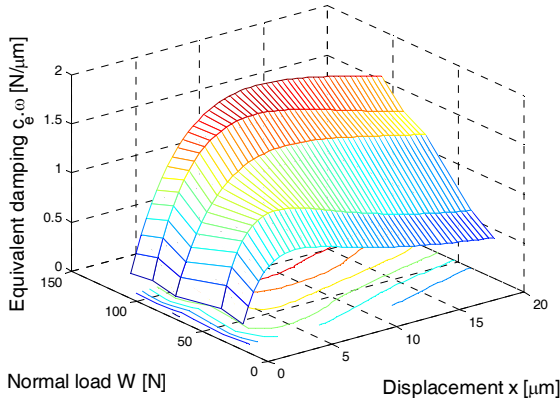


Fig. 14. Equivalent damping as a function of normal load and displacement

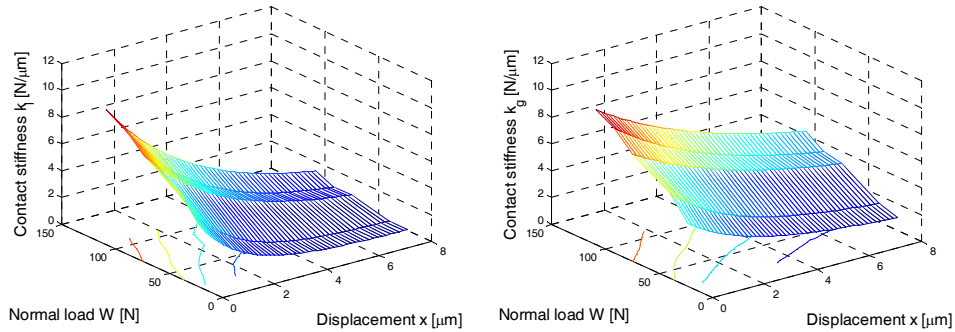


Fig. 15. Local and global stiffness as a function of normal load and displacement

3.3. Experimental results for steel on steel

The experimental results for steel on steel prove that the system is not powerful enough to perform the friction identification in pre-sliding regime as a function of the load conditions. Due to the limitation in the power of the actuator only a small portion of the hysteresis that can be seen as a pure stiffness could be identified. The highest damping is observed at the lowest load.

In Fig. 16, some hysteresis data of the two bodies and the relative displacement of them and, separately the fit of the relative displacement hysteresis are plotted for one normal load $W=75$ N. It can be seen that for higher loads there is not hysteresis loop due to the stiffness in the contact that is increasing with the normal load. However, the evolution of the parameters h_0 and a_c shows similar trend with higher values for h_0 and lower values for a_c compared with the studied material contacts (Fig. 17).

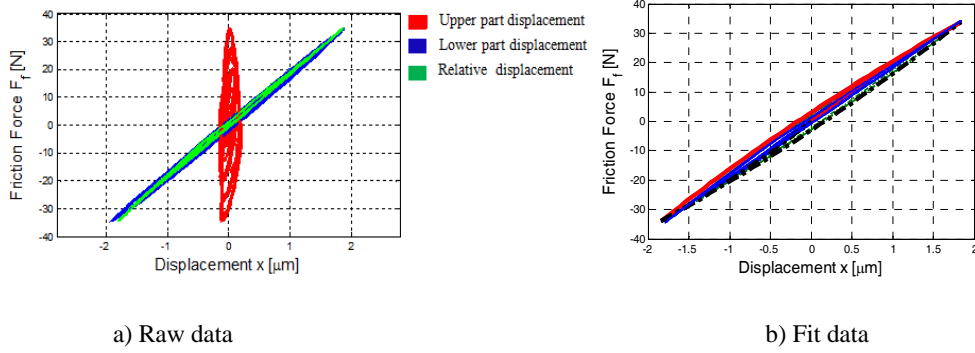


Fig. 16. Hysteresis in pre-sliding regime: $W = 75$ N, $f = 1$ Hz; a) raw data; b) fit data

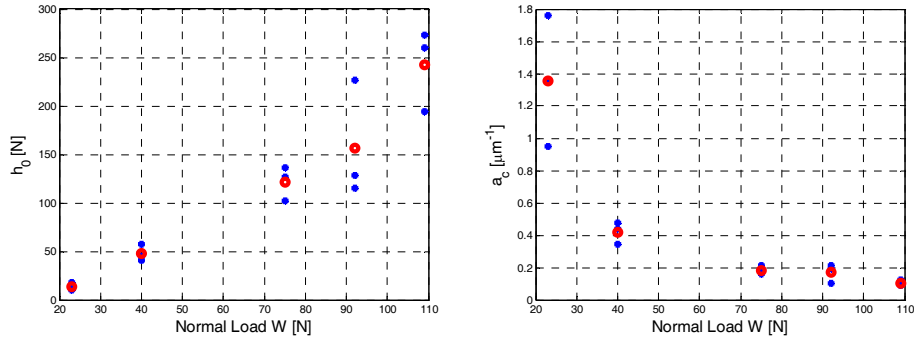


Fig. 17. Evolution of the hysteresis parameters as a function of the normal load for steel on steel contact

In Fig. 18 is presented the pre-sliding distance as a function of the normal load that has a similar trend. The values for the pre-sliding distance are much higher than for other material. In Fig. 19 is presented the equivalent damping $c_e \cdot \omega$ as a function of the normal load and displacement. The global contact stiffness and local contact stiffness are shown in Fig. 20.

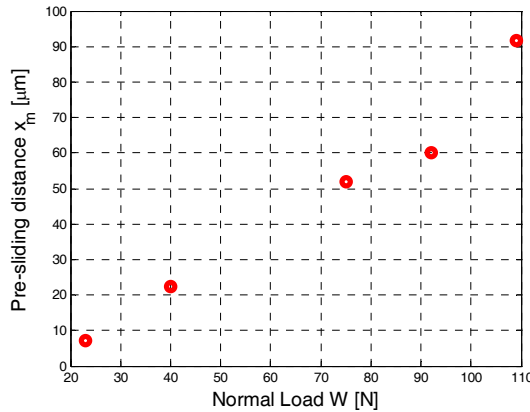


Fig. 18. Evolution of the pre-sliding distance as a function of the normal load for steel on steel

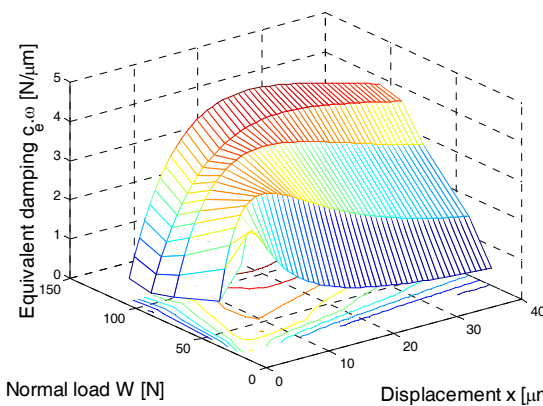


Fig. 19. Equivalent damping as a function of normal load and displacement

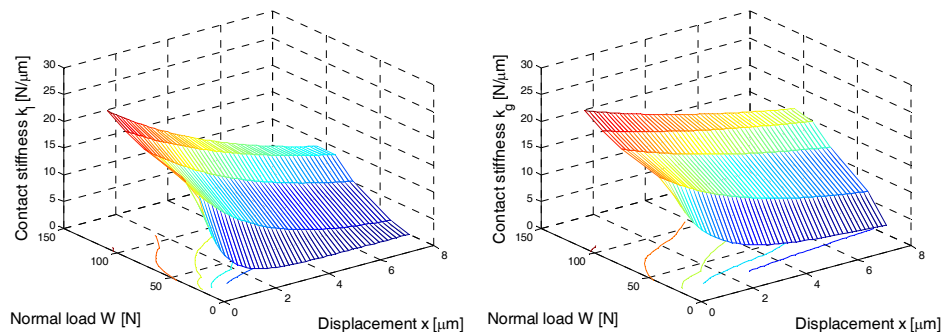


Fig. 20. Local stiffness and global stiffness as a function of normal load and displacement

4. Conclusions

In this paper, an existing friction model is used to determine the frictional characteristic of three different contact materials in a flat on flat configuration. For this type of configuration, the friction force as a function of the displacement and normal load was investigated. A typical hysteresis behaviour for the aluminium and plastic contact was observed which is material, normal load and displacement, amplitude dependent. Due to the limitations in force of actuator and hardness of steel, only a small portion of the loop could be identified, therefore the parameter identification of the model parameters could not be correctly determined. However, the trend is the same as for the other two contact materials, e.g. aluminum and PVC.

The experimental results were described, in which the evolution of the friction coefficient and friction force as a function of the normal load and displacement is presented. The friction hysteresis curve was determined by two parameters, which describe the curvature of the hysteresis curve and the saturation value. The increased saturation value with the normal load seems to be non-linear due to the frictional contact. The pre-sliding distance, decreases with increasing normal load.

The contact stiffness and equivalent contact damping are determined from the virgin curve expression. For all material contacts, the contact stiffness is increasing with the load and weakening with the displacement and equivalent contact damping is increasing with the increasing normal load and displacement. The behaviour of the frictional contact is necessary in order to predict and to control the performance of mechanical structures. The experimental investigation is performed in order to understand the behaviour of frictional contact. The experimental results will be used to develop a theoretical model of the tangential contact stiffness of flat on flat frictional contacts.

Acknowledgements

The work has been funded by the Sectoral Operational Programme Human Resources Development 2007-2013 of the Romanian Ministry of Labour, Family and Social Protection through the Financial Agreement POSDRU/88/1.5/S/60203. Thanks go to the Department of Mechanical Engineering, Division Production engineering, Machine design and Automation, from the KU Leuven, which made possible to perform the experiments.

R E F E R E N C E S

- [1] *J. Wojewoda, A. Stefanski, M. Wiercigroch and T. Kapitaniak*, Hysteretic effects of dry friction: modelling and experimental studies, *Phil. Trans. R. Soc. A*, vol. 366, 2008, pp. 747-765
- [2] *D. Rizos and S. D. Fassois*, Presliding friction identification based upon the Maxwell Slip model structure, in *Chaos* vol. 14, no. 2, June 2004 pp. 431-445
- [3] *H. S. Benabdallah*, Static friction coefficient of some plastics against steel and aluminum under different contact conditions, *Tribology International* vol. 40, 2007, pp. 64-73
- [4] *F. Al-Bender, W. Symens, J. Swevers, H. Van Brussel*, Theoretical analysis of the dynamic behavior of hysteresis elements in mechanical systems, *International Journal of Non-Linear Mechanics*, vol. 39, 2004, pp. 1721 – 1735
- [5] *B. M. Y. Nouri*, Friction identification in mechatronic systems, *ISA Transactions* vol. 43, 2004, pp. 205-216
- [6] *P. J. Blau*, The Significance and Use of the Friction Coefficient, *Tribol. Int.*, vol. 34, 2001, pp. 585-591
- [7] *J.A. Greenwood and J.B.P. Williamson*, The contact of nominally flat surfaces, *Proc. Roy. Soc. Lond. Vol. 295*, 1966, pp. 300-319
- [8] *M.T. Bengisu and A. Akay*, Relation of dry-friction to surface roughness. – *Journal of Tribology*, vol.119, 1997, pp.18-25.
- [9] *J. A. Abdo and K. Farhang*, Theoretical Modeling and Experimental Technique to Study of Contact Load Ratio – Friction Function, *15th ASCE Engineering Mechanics Conference* June 2-5, 2002, Columbia University, New York, NY
- [10] *B. Bhushan, A. V. Kulkarni*, Effect of normal load on microscale friction measurements, *Thin Solid Films*, vol. 278, 1996, pp. 49-56
- [11] *J.A. Abdo*, Experimental technique to study tangential to normal contact load ratio, *Tribology Transactions*, vol.48, 2005, pp 356-365
- [12] *V. Lampaert, F. Al-Bender, J. Swevers*, Experimental characterisation of dry friction at low velocities on a developed tribometer setup for macroscopic measurements, *Tribology Letters*, vol. 16 (1-2), 2004, pp. 95-105
- [13] *Thierry Janssens*, Dynamic characterization and modeling of dry and lubricated friction for stabilization and control purposes, *Katholieke University Leuven*, PhD thesis, 2010
- [14] *K. De Moerlooze, F. Al-Bender*, On the relationship between normal load and friction force in pre-sliding frictional contacts. Part 2: Experimental investigation, *Wear*, vol. 269, 2010, pp. 183-189